Photo: Fiamma Straneo (WHOI)

Timing and characterization of glacier calving events from surface waves

Clark Richards (crichards@whoi.edu) and Fiamma Straneo (fstraneo@whoi.edu)
Woods Hole Oceanographic Institution
266 Woods Hole Rd. MS#21, Woods Hole, MA 02543 USA

Photo: Sarah Das (WHOI)

1. Introduction

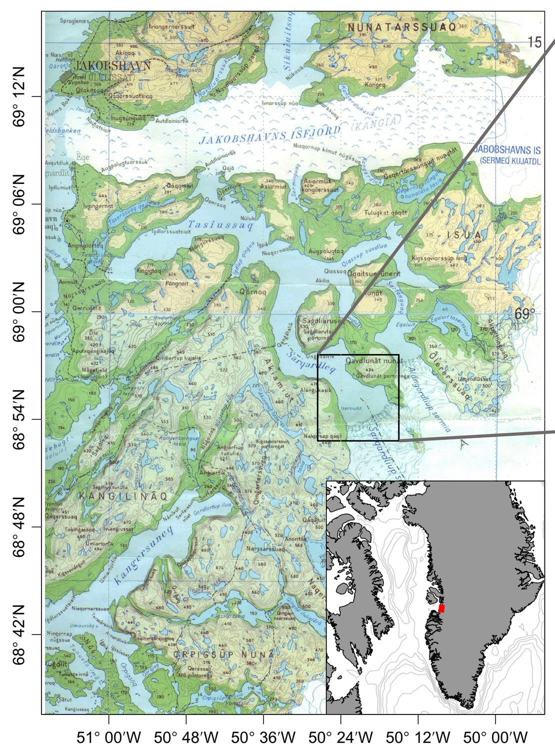

Figure 1: Map showing location of study area (black rectangle), to the south of Jakobshavn Icefjord

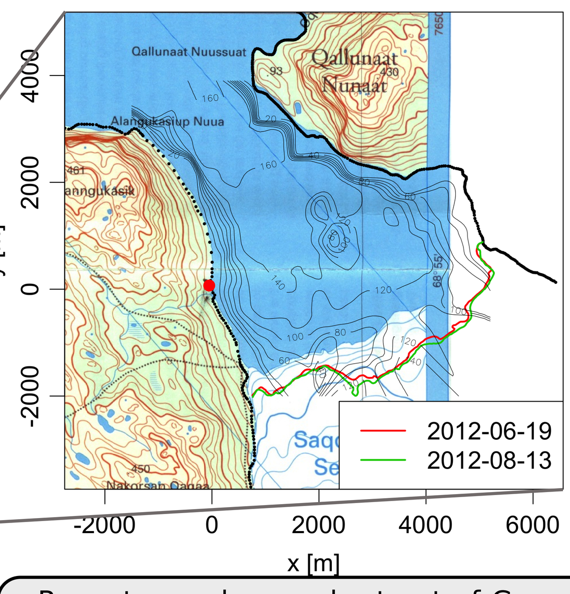

Figure 2: Detail of study region. Bathymetry is indicated by the black contours, and two positions of the glacier face are indicated by the red and green lines (thanks to I. Joughin). The red circle marks the location of the submerged pressure sensor.

Recent speed up and retreat of Greenland's tidewater glaciers has lead to increased interest in mechanisms occurring at the glacier margin. The role played by changes in glacier calving is not well understood - largely due to a lack of observations of when and where calving events occur.

Here, we describe a simple method for detecting glacier calving events by tracking the excited surface waves using a submerged pressure sensor. Data collected this pilot study indicates that the method can be used to reconstruct both the timing and localization of the event along the glacier face.

2. Data

• ***Saquardliup glacier*** is 5 km wide (Figure 1), grounded at ~100 m, which is relatively stable and calves small pieces of ice frequently.

• A single pressure sensor was deployed in ~1.25 m of water near the shore, sampling at 1 Hz for 7 days. The raw pressure time series shows tidal variations (too short for a proper tidal analysis), with high frequency surface wave events superimposed (Figures 3 and 4). Tidal range is ~2 metres.

• Pressure residual (gray line in Figure 3) shows surface wave events, most likely triggered by ice calving. Largest amplitude events occur at low tide, either due to wave breaking in shallow water, or increased calving from glacier destabilization.

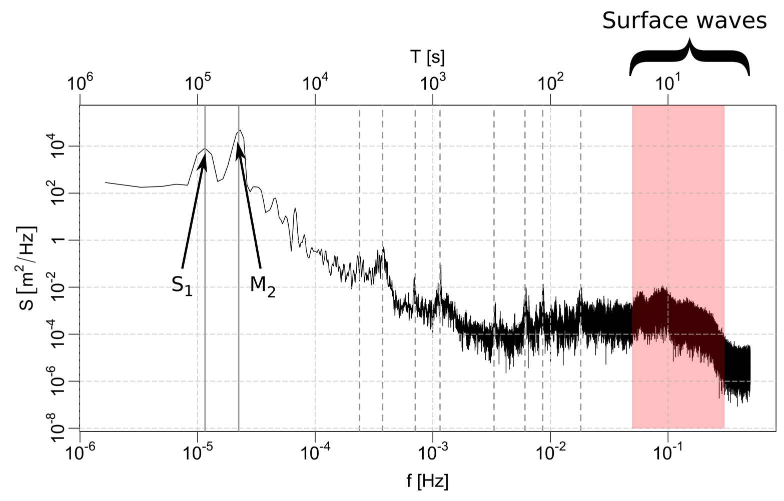

Figure 4: Spectrum of pressure time series. Vertical lines indicate notable frequencies, including: S_1 and M_2 (solid), various seiche modes (dashed), and the high frequency surface wave band of interest here (red).

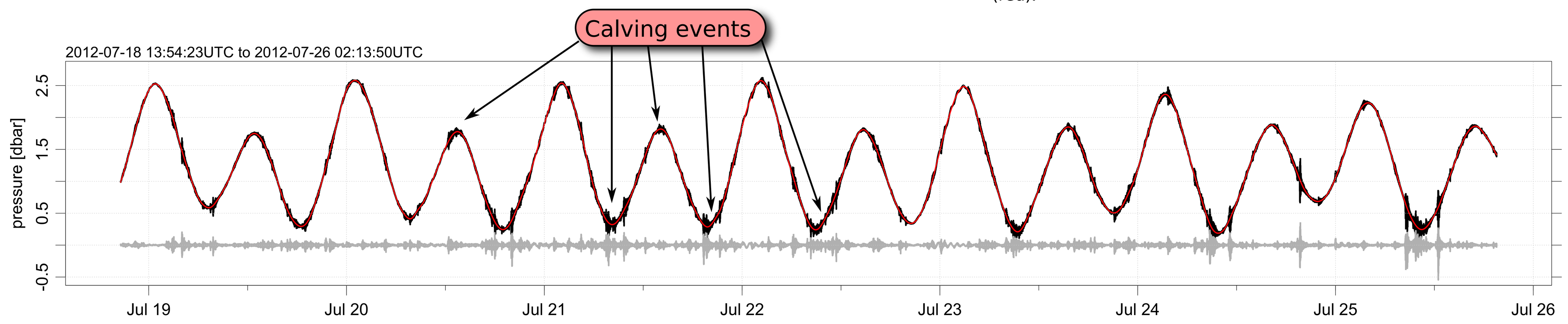

Figure 3: Raw pressure time series (black), tidal fit using a smoothing spline (red), and the pressure residual (gray) showing episodic wave events with wave amplitudes of up to 20 to 30 cm.

3. Data Analysis

• After removing tidal and low frequency signals with a smoothing spline, a spectrogram was constructed using a short-time Fourier transform.

• We expect calving events to be revealed as distinctive sloped bands (see e.g. MacAyeal *et al.* 2009), indicating the arrival of dispersive surface wave trains (Section 4). The dispersion is highly linear, suggesting that it results from deep water waves.

• Seiche events with periods of ~50 minutes are also observed in the time series, with calving events superimposed on the ~10 cm signal (Figure 6, at right). The cause of the seiches (local or remote calving, wind, shelf forcing, etc) is unknown at this time.

Figure 6: Detail of spectrogram and time series during seiche event. Peak to peak amplitude of seiche is ~10 cm, with a dominant period of ~50 minutes.

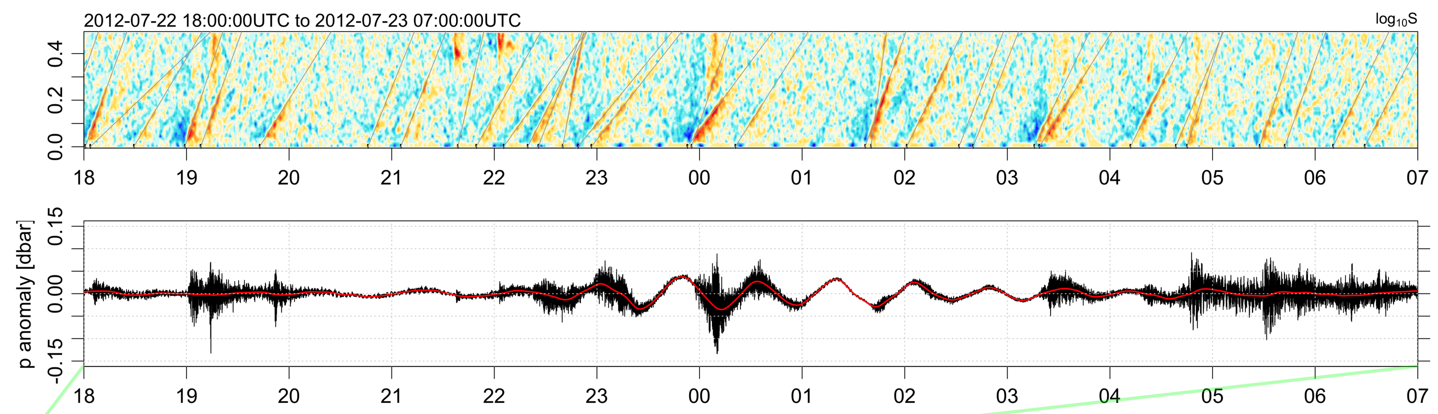

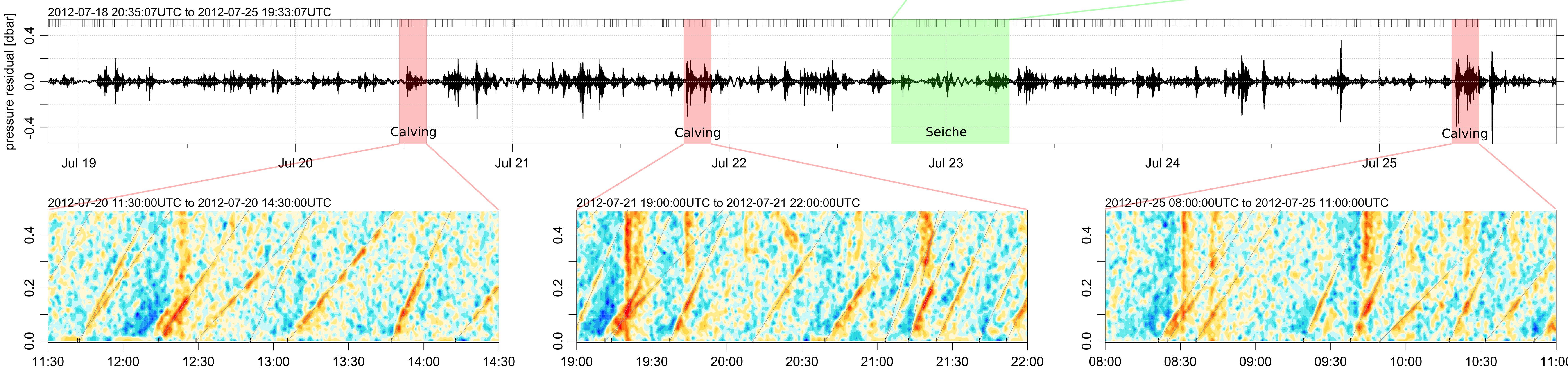

Figure 5: Spectrograms of three different 3 hour periods (red regions in top plot), showing the arrival of linearly dispersive wave trains. Sloped dark gray lines indicate manual detection and linear fitting of *df/dt* (see Section 4). The green region highlights a period of significant seiche activity, with an expanded plot in Figure 6, for which the cause is unknown.

4. Calving location

In deep water, surface waves follow the dispersion relation:

$$\omega^2 = gk$$

where ω is the angular frequency and k is the wavenumber. The group velocity for a particular k is then

$$c_g = \frac{\partial \omega}{\partial k} = \frac{1}{2}\sqrt{\frac{g}{k}}$$

An expression for the distance from the wave source Δ can be derived based on the observed dispersion df/dt as:

$$\boxed{\Delta = \frac{g}{4\pi(df/dt)}}$$

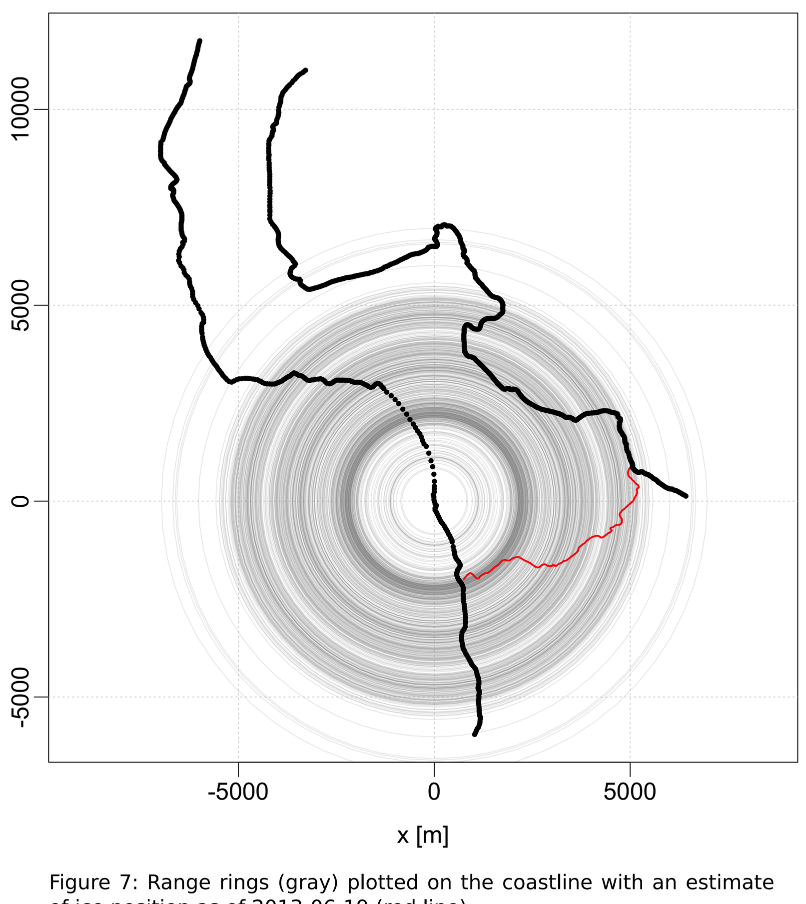

Figure 7: Range rings (gray) plotted on the coastline with an estimate of ice position as of 2013-06-19 (red line).

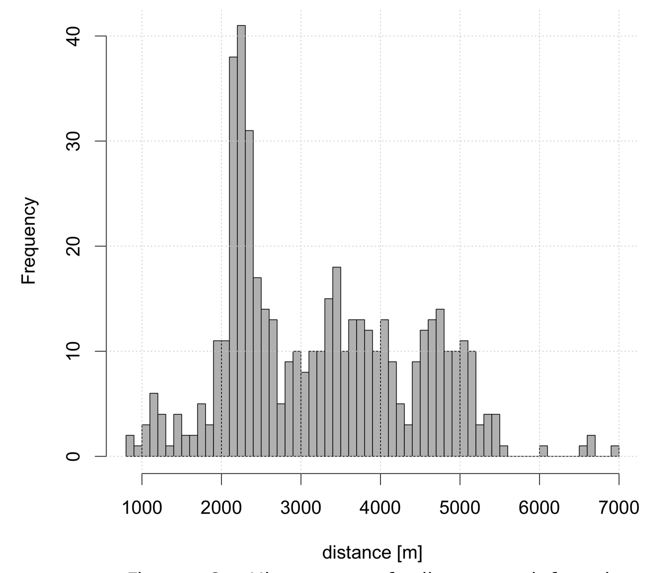

Figure 8: Histogram of distances inferred using Equation 3 Note the large peak between 2000 and 2500 m.

• Calving events were detected manually from the spectrogram (Figure 5).

• The average calving rate over the experiment was **2.92 events/hour**.

• Calving occured along the entire face of the glacier, however the most active region of ice loss was between **2000 and 2500 m** (Figure 8) from the sensor.

5. Future work

1. Better understanding of bathymetry and wave propagation characteristics (rebounds, shallow/intermediate depth dispersion, etc.)

2. Planned second deployment in July/August 2013:

• 2 - 3 pressure sensors at all times for better triangulation.

• Deployment of a shore-based camera (see e.g. Bourgault 2008) for time-lapse monitoring of the ice face as well as visible surface features and near-surface currents (Figure 9).

• Comparison with passive acoustic detection of calving events.

3. Longer term deployments (several months).

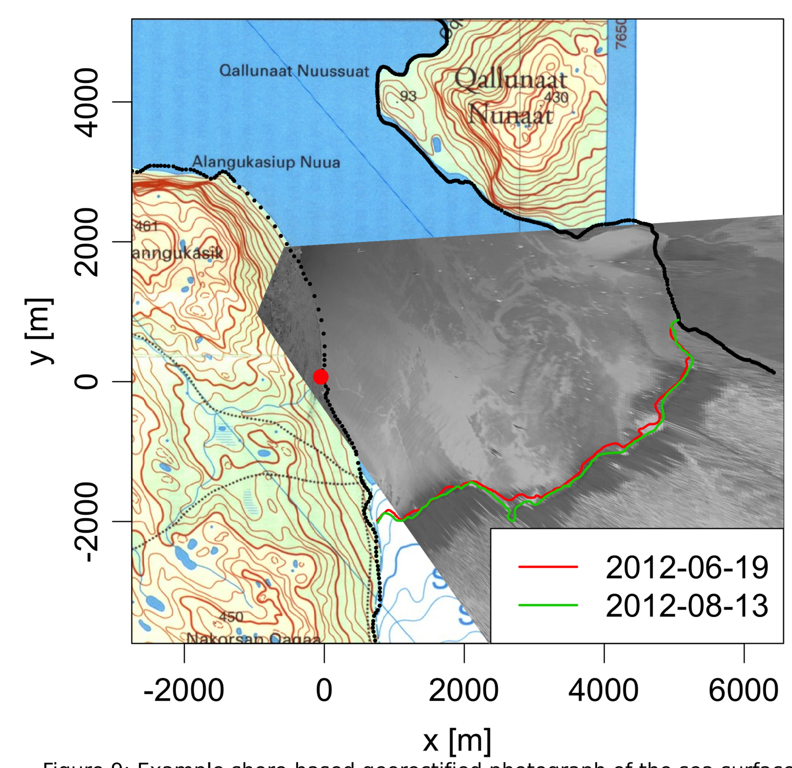

Figure 9: Example shore-based georectified photograph of the sea surface, highlighting visible surface features (such as ice, sediments, and surface waves). A time-lapse series of such images will be used to monitor the glacier face, as well as track floating ice to infer horizontal velocities.

References

1. D. Bourgault. Shore-based photogrammetry of river ice. Canadian Journal of Civil Engineering, 35(1):80– 86, 2008.

2. D. R. MacAyeal, E. A. Okal, R. C. Aster, and J. N. Bassis. Seismic observations of glaciogenic ocean waves (micro-tsunamis) on icebergs and ice shelves. Journal of Glaciology, 55(190):193–206, 2009.

Acknowledgements

Funding for the field program was provided by the WHOI Arctic research Initiative.

We would like to thank R. Jackson, J. Pietro, and S. Das for their help in the 2012 field campaign.